

1 **Efficacy of Host Cell Serine Protease Inhibitor MM3122 against SARS-CoV-2 for**
2 **Treatment and Prevention of COVID-19**

3

4

5 Adrianus C.M. Boon^{1,*}, Traci L.Bricker¹, Ethan J. Fritch², Sarah R. Leist³, Kendra Gully³, Ralph
6 S. Baric³, Rachel L. Graham³, Brigid V. Troan⁴, Matthew Mahoney⁵, James W. Janetka^{5,*}

7

8 ¹Department of Medicine, Washington University School of Medicine, Saint Louis MO 63110,
9 USA

10 ²Department of Microbiology and Immunology, School of Medicine, University of North Carolina
11 at Chapel Hill

12 ³Department of Epidemiology, Gillings School of Global Public Health, University of North
13 Carolina, Chapel Hill, NC 27599, USA

14 ⁴Inotiv, West Lafayette, IN 47906 USA

15 ⁵Department of Biochemistry and Molecular Biophysics, Washington University School of
16 Medicine, Saint Louis MO 63110, USA

17

18 * Corresponding authors

19 Adrianus Boon (jboon@wustl.edu), Washington University School of Medicine, 660 S Euclid
20 Avenue, Campus Box 8051, St Louis MO 63110 USA.

21 or

22 James Janetka (janetkaj@wustl.edu), Washington University School of Medicine, 660 S Euclid
23 Avenue, Campus Box 8231 St Louis MO 63110 USA.

24 **ABSTRACT**

25 We have developed a novel class of peptidomimetic inhibitors targeting several host cell
26 human serine proteases including transmembrane protease serine 2 (TMPRSS2), matriptase and
27 hepsin. TMPRSS2 is a membrane associated protease which is highly expressed in the upper
28 and lower respiratory tract and is utilized by SARS-CoV-2 and other viruses to proteolytically
29 process their glycoproteins, enabling host cell receptor binding, entry, replication, and
30 dissemination of new virion particles. We have previously shown that compound MM3122
31 exhibited sub nanomolar potency against all three proteases and displayed potent antiviral effects
32 against SARS-CoV-2 in a cell-viability assay. Herein, we demonstrate that MM3122 potently
33 inhibits viral replication in human lung epithelial cells and is also effective against the EG.5.1
34 variant of SARS-CoV-2. Further, we have evaluated MM3122 in a mouse model of COVID-19
35 and have demonstrated that MM3122 administered intraperitoneally (IP) before (prophylactic) or
36 after (therapeutic) SARS-CoV-2 infection had significant protective effects against weight loss
37 and lung congestion, and reduced pathology. Amelioration of COVID-19 disease was associated
38 with a reduction in pro-inflammatory cytokines and chemokines production after SARS-CoV-2
39 infection. Prophylactic, but not therapeutic, administration of MM3122 also reduced virus titers in
40 the lungs of SARS-CoV-2 infected mice. Therefore, MM3122 is a promising lead candidate small
41 molecule drug for the treatment and prevention of infections caused by SARS-CoV-2 and other
42 coronaviruses.

43

44 **IMPORTANCE**

45 SARS-CoV-2 and other emerging RNA coronaviruses are a present and future threat in
46 causing widespread endemic and pandemic infection and disease. In this paper, we have shown
47 that the novel host-cell protease inhibitor, MM3122, blocks SARS-CoV-2 viral replication and is
48 efficacious as both a prophylactic and therapeutic drug for the treatment of COVID-19 in mice.
49 Targeting host proteins and pathways in antiviral therapy is an underexplored area of research

50 but this approach promises to avoid drug resistance by the virus, which is common in current
51 antiviral treatments.

52

53 **INTRODUCTION**

54 The COVID-19 pandemic, caused by the Severe Acute Respiratory Syndrome Coronavirus 2
55 (SARS-CoV-2), has illuminated the devastating impact of new emerging viral diseases on both
56 the global economy and health of populations¹. It has affected all aspects of human life and
57 highlighted the threat of future outbreaks with other respiratory viruses for which currently
58 available drugs will be ineffective. Incredibly, vaccines as well as several new drug candidates
59 targeting this virus were developed at unprecedented speed because of early countermeasure
60 work that focused on paradigm pathogens within the coronavirus family²⁻⁴. This was made
61 possible by the combined efforts of scientists worldwide who elucidated details about the makeup
62 and pathogenesis of SARS-CoV-2 infection. This work also resulted in the identification of several
63 potential therapeutic targets such as the viral entry receptor, angiotensin converting enzyme 2
64 (ACE2), and host cell proteases, such as transmembrane protease serine 2 (TMPRSS2) and
65 cathepsin L1 (CTSL1), required for entry, replication, and release of the virus⁵⁻⁸.

66 TMPRSS2⁹⁻¹¹ has a trypsin-like serine protease domain and belongs to the family of Type II
67 Transmembrane Serine Protease (TTSP) proteolytic enzymes with reported physiological roles
68 in cancer and many other diseases¹²⁻¹⁵. TMPRSS2 has previously been shown to be important in
69 other coronavirus infections caused by SARS-CoV-1^{16, 17}, HKU-1¹⁸, MERS-CoV¹⁹, and others^{20,}
70 ²¹. Furthermore, both TMPRSS2 and the other TTSPs, matriptase (ST14)^{22, 23} and HAT (human
71 airway trypsin-like protease, TMPRSS11D)^{24, 25}, have been demonstrated to proteolytically
72 process the hemagglutinin (HA) protein on the surface of some influenza A viruses and SARS-
73 CoV-1¹⁷, allowing viral cell adhesion and entry in these infections^{24, 26-31}. Additionally, TMPRSS2
74 was found to support replication of other respiratory viruses including human para-influenza virus

75 type 1, 2 and mouse Sendai virus³². This makes TMPRSS2 an excellent target for the
76 development of a broadly acting antiviral inhibitor³³ against diverse respiratory viruses^{24, 34-39}.

77 We recently reported on the discovery and development of a new class of peptidomimetic
78 TMPRSS2 inhibitors³⁹. These inhibitors were rationally designed based on the peptide substrate
79 sequence specificity of TMPRSS2¹⁵ and molecular docking studies using the X-ray structure of
80 TMPRSS2 bound to another inhibitor nafamostat^{40, 41}. These inhibitors, including MM3122 and
81 MM3144, are significantly more potent than another reported TMPRSS2 inhibitor Camostat⁴¹,
82 suggesting improved efficacy *in vivo*. Unlike MM3122, which has the desired selectivity for
83 TMPRSS2 over the coagulation serine proteases thrombin and Factor Xa, MM3144 does not.
84 This compound was subsequently reported as a matriptase and TMPRSS2 inhibitor by another
85 group as N-0386⁴². We tested the *in vitro* and *in vivo* efficacy of the most promising compound at
86 the time, MM3122, in Calu-3 human lung epithelial cells and in a mouse model of SARS-CoV-2.
87 Overall, we showed potent antiviral efficacy of MM3122 against XBB.1.5 and EG.5.1 variant of
88 SARS-CoV-2 *in vitro* and amelioration of COVID-19 disease *in vivo*.

89

90 RESULTS

91 **MM3122 inhibits authentic SARS-CoV-2 replication in human lung epithelial cells.** The
92 ability of MM3122, a TMPRSS2 inhibitor, to inhibit wild-type (wt) SARS-CoV-2 infection and
93 replication was assessed on Calu-3 cells, a human lung epithelial cell line. At a 0.03 μ M
94 concentration of MM3122, virus replication was completely inhibited, and no infectious virus was
95 detected in the supernatant of the treated and SARS-CoV-2 infected cells (**Fig 1**). The inhibitory
96 concentration (IC_{50}) of MM3122 was \sim 0.01-0.02 μ M against the authentic wt SARS-CoV-2 virus.
97 This is greater than 50 times more potent than Remdesivir which had an IC_{50} of \sim 1 μ M, an RNA-
98 dependent RNA polymerase inhibitor developed for other viral infections that is one of the FDA-
99 approved drugs approved to treat SARS-CoV-2 infected patients⁴³. MM3122 was also tested for
100 its activity against the EG.5.1 variant of SARS-CoV-2. Similar to wt SARS-CoV-2, we observed

101 robust inhibition of the virus with an IC₅₀ of ~0.05-0.1 μM. Taken together, these studies
102 demonstrate the high potential for small molecule TMPRSS2 inhibitors to inhibit replication of
103 SARS-CoV-2 and several of its many variants.

104 **MM3122 is a multi-targeted serine protease inhibitor with activity against some**
105 **cathepsins.** To determine the target specificity of MM3122 for TMPRSS2, we tested for its
106 inhibitory activity against 53 serine and cysteine proteases (**Table 1**). In our previous paper³⁹, we
107 profiled MM3122 for its inhibition of hepatocyte growth factor activator (HGFA), matriptase,
108 hepsin, thrombin, and Factor Xa. For the 47 other proteases we contracted Reaction Biology Co.
109 (Malvern, PA) to determine the IC₅₀ values of MM3122 against a large panel of serine and cysteine
110 proteases of high importance. A previous group had reported the selectivity profile for Camostat
111 and Nafamostat against these same proteases⁴⁴ which is also shown in **Table 1**. In addition to
112 TMPRSS2, MM3122 has potent activity (0.01 to 10 nM) against only 7 other proteases,
113 matriptase, hepsin, matriptase-2, plasma kallikrein, trypsin, tryptase b2 and tryptase g1. It has
114 moderate inhibitory activity (10 nM to 1 μM) against HGFA, Factor Xa, kallikrein 1 (KLK1), KLK5,
115 KLK14, plasmin, and proteinase K and surprisingly against the cysteine protease cathepsin S with
116 an IC₅₀ of 590 nM. Furthermore, MM3122 also inhibited the other cysteine proteases cathepsin
117 C, cathepsin L and papain, with IC₅₀s of 1.4 μM, 12.8 μM, and 1.1 μM. Comparing the selectivity
118 profile of MM3122 to that of Camostat and Nafamostat reveals that the cysteine protease activity
119 is absent in the latter. Otherwise, the profiles are generally similar with some exceptions, notably
120 decreased activity of MM3122 against thrombin, plasmin, Factor VIIA and XIA, KLK12, KLK13
121 and KLK14, urokinase, matriptase-2, trypsin and the 2 tryptases. We also found that MM3122
122 does not inhibit furin or the SARS-CoV-2 proteases, M_{pro} and PL_{pro}.

123 **MM3122 ameliorates SARS-CoV-2 induced disease in mice.** To assess the antiviral activity
124 of MM3122 *in vivo*, four groups of mice were treated with 50 mg/kg or 100 mg/kg MM3122 30
125 minutes prior to (prophylactic) and 24 hours after (therapeutic) intranasal infection with the MA10
126 strain of SARS-CoV-2. A mock infected and vehicle treated group were included as controls.

127 Intranasal inoculation of vehicle treated mice with SARS-CoV-2 resulted in significant weight loss
128 compared to mock infected animals (**Fig 2A**). Importantly, none of the MM3122 groups lost any
129 significant amount of body weight. Five days after infection, lung congestion was assessed using
130 an independently developed scoring system as described in the Methods. Vehicle-treated mice
131 that were infected with SARS-CoV-2 MA10 demonstrated evidence of congestion with scores
132 ranging from 1-3. These scores were reduced to 0 for infected mice that received 50 and 100
133 mg/kg MM3122 prophylactically ($P < 0.01$), and 0.5 for mice that received 50 and 100 mg/kg
134 MM3122 therapeutically. Mice that received MM3122 prior to infection also had reduced virus
135 titers (5000-10,000-fold) compared to vehicle treated and infected animals (**Fig 2B**). However,
136 mice that received MM3122 24 h after infection had similar amounts of virus in the lungs compared
137 to the vehicle treated animals. Finally, we performed pathological analysis of the lungs of MM3122
138 and control treated mice. Global pneumonia, used to assess the % of lung affected, was between
139 3 (>50%) and 4 (>80%) for the SARS-CoV-2 infected and vehicle treated mice. This score was
140 reduced to 1.2 ($P < 0.05$) and 1.6 in the mice that received 50 mg/kg and 100 mg/kg of MM3122
141 prior to virus infection. No change in the global pneumonia score was observed for the mice that
142 received 50 (score = 3) and 100 (score = 3.2) mg/kg of MM3122 after virus infection. Similarly,
143 the bronchointerstitial pneumonia score was reduced in the animals that received MM3122 prior
144 to infection (1.2 and 1.5 for 50 mg/kg ($P < 0.05$) and 100 mg/kg respectively) but not after SARS-
145 CoV-2 infection. Finally, vasculitis and endotheliitis replicated control baseline levels (average
146 score = 0.3) in the prophylactically treated group (score = 0.4 and 0.3 for 50 mg/kg and 100 mg/kg
147 respectively). A reduction in score was also observed for the mice that received MM3122 after
148 infection (score = 1.2 and 1.8 for 50 mg/kg and 100 mg/kg respectively), but this was not
149 statistically significant compared to the infected and vehicle control treated animals (score = 2.8).

150 **MM3122 reduces inflammatory cytokine and chemokine production after SARS-CoV-2**
151 **infection.** Weight loss and severe disease after SARS-CoV-2 infection is associated with
152 exacerbated inflammatory responses resulting in lung congestion and immunopathology. To

153 assess inflammation, cytokine and chemokine concentrations were quantified in lung tissue
154 homogenates using a mouse cytokine 23-plex assay. Compared to uninfected and vehicle control
155 animals, the levels of IL-6, KC, G-CSF, CCL2, CCL3, CCL4, IL1 alpha, IL-12p40 and CCL5 were
156 increased three-fold or more five days after infection with the MA10 strain of SARS-CoV-2 (**Fig**
157 **3**). Prophylactic and therapeutic treatment with MM3122 significantly ($P < 0.001$) reduced the
158 amount of IL-6, KC, G-CSF, CCL2 and CCL3 in the lungs of these mice. Smaller reductions in
159 cytokine and chemokine productions were observed for CCL4, IL-1 alpha, IL-12p40, and CCL5.
160 Combined, these data show that the TMPRSS2 inhibitor MM3122 reduces virus titers and
161 inflammation after SARS-CoV-2 infection.

162

163 **DISCUSSION**

164 The COVID-19 pandemic began 4 years ago and is still a major economic catastrophe and
165 medical problem worldwide costing over \$14 trillion in economic losses in the US⁴⁵ and resulting
166 in excess mortality rates estimated at exceed 24 million people worldwide through early 2023⁴⁶.
167 While highly efficacious vaccines have saved millions of lives globally⁴⁷, they are not 100%
168 effective, even less so for variants, and a large percentage of the population refuses to be
169 vaccinated so there is a dire need for new drugs to prevent and treat this life-threatening disease.
170 There are some small molecule FDA-approved drugs to treat COVID-19¹ including the viral
171 polymerase inhibitors remdesivir and molnupiravir, as well as SARS-CoV-2 Mpro protease
172 inhibitor nirmatrelvir, sold under the brand name Paxlovid. With the exception immunomodulatory
173 treatments for COVID-19 such as the JAK1/JAK2 inhibitor baricitinib⁴⁸⁻⁵⁰, which target the
174 symptoms of infection and not viral pathogenesis directly, there are no approved antiviral drugs,
175 which target the host and confer protection against multiple different viruses from diverse viral
176 families. Concomitantly, others, and we have reported on the first potential drugs, targeting the
177 TMPRSS2 and matriptase, to treat SARS-CoV-2 and COVID-19^{39, 42}. TMPRSS2, and other host
178 cell transmembrane proteases⁵¹ including matriptase are essential for viral entry of many

179 respiratory RNA viruses into the lung tissue. In this communication, we have demonstrated that
180 one lead candidate drug that we have developed, MM3122, exhibited significant protective effects
181 against weight loss, lung congestion (gross lung discoloration), and inflammation administered
182 prophylactically at both low and high doses, in aged mice infected with mouse-adapted SARS-
183 CoV-2. These effects were less pronounced in the therapeutic groups. Interestingly, these
184 protections did not fully correspond with protection from viral replication, as titers were lower or
185 absent in the prophylactic group but were not significantly different from the infected vehicle
186 control in the therapeutic group. These protective effects of COVID-19 in the lung can potentially
187 be explained by inhibition of the proteolytic activation of other substrates by TMPRSS2,
188 matriptase, and hepsin or the other proteases, which MM3122 targets such as tryptase (**Table 1**).
189 In summary, these promising results suggest MM3122 is a potential clinical candidate for the
190 treatment and prevention of diseases including COVID-19, caused from infection by SARS-CoV-
191 2 and other coronaviruses.

192 **Limitations of the study.** We note several limitations of our study. (a) The *in vivo* efficacy of
193 MM3122 was not tested against more recent variants of SARS-CoV-2 in mice or in Syrian
194 hamsters. For the latter, we will need to perform PK studies, which is beyond the scope of this
195 study. Also, the more recent variants of SARS-CoV-2 are attenuated compared to MA10 strain of
196 SARS-CoV-2, creating challenges in observing effects on weight loss and disease of MM3122.
197 Also, given that MM3122 has similar activity against EG.5.1 *in vitro*, we do not expect differences
198 *in vivo*. (b) We did not evaluate the efficacy of MM3122 in male mice. Males are considered more
199 susceptible to SARS-CoV-2 infection and therefore we expect more disease in the untreated
200 animals with continued amelioration of disease in the MM3122 treated animals. (c) To increase
201 efficacy, we are currently working on developing improved compounds with longer half-life and
202 higher compound exposure compared to MM3122.³⁹ One potential way to achieve increased
203 efficacy with MM3122 would be to develop formulations for inhalation or nebulization as
204 alternative administration routes, which would deliver compound directly to the respiratory tract at

205 the primary site of viral entry and the infection. In summary, these studies demonstrate that
206 MM3122 is effective in inhibiting SARS-CoV-2 replication *in vitro* and that administration of
207 MM3122 *in vivo* reduces COVID-19 disease in mice.

208

209 **MATERIALS AND METHODS**

210 ***Cells and Viruses.*** Vero cells expressing human angiotensin converting enzyme 2 (ACE2)
211 and transmembrane protease serine 2 (TMPRSS2) (Vero-hACE2-hTMPRSS2^{52, 53}, gift from Adrian
212 Creanga and Barney Graham, NIH) were cultured at 37°C in Dulbecco's Modified Eagle medium
213 (DMEM) supplemented with 10% fetal bovine serum (FBS), 10 mM HEPES (pH 7.3), 100 U/mL of
214 Penicillin, 100 µg/mL of Streptomycin, and 10 µg/mL of puromycin. Vero cells expressing
215 TMPRSS2 (Vero-hTMPRSS2)⁵³ were cultured at 37°C in DMEM supplemented with 10% fetal
216 bovine serum (FBS), 10 mM HEPES (pH 7.3), 100 U/mL of Penicillin, 100µg/mL of Streptomycin,
217 and 5 µg/mL of blasticidin. Calu-3 cells were cultured in DMEM media supplemented with 1.0 mM
218 sodium pyruvate, non-essential amino-acids (NEAA), 100 U/mL of penicillin, 100 µg/mL
219 streptomycin, 2.0 mM L-glutamine, 10 mM HEPES, and 10% Fetal Bovine Serum (FBS).

220 The Lineage A variant of SARS-CoV-2 (WA1/2020), or the XBB.1.5 and E.G.5.1 (from Mehul
221 Suthar) variants of SARS-CoV-2 were propagated on Vero-hTMPRSS2 cells. The virus stocks
222 were subjected to next-generation sequencing, and the S protein sequences were identical to the
223 original isolates. The infectious virus titer was determined by plaque and focus-forming assay on
224 Vero-hACE2-hTMPRSS2 or Vero-hTMPRSS2 cells.

225 Baric laboratory-generated stock of SARS-CoV-2 MA10, a mouse-adapted virulent mutant
226 generated from a recombinantly derived synthesized sequence of the Washington strain that
227 causes severe acute and chronic disease in mice^{54, 55}. Virus was maintained at low passage (P2-
228 P3) to prevent the accumulation of additional potentially confounding mutations.

229 ***Drug Preparation and Administration.*** MM3122³⁹ was freshly prepared at 8 mg/mL in 5%
230 DMSO in PBS. MM3122 was administered intraperitoneal (IP) at 50 and 100 mg/kg bodyweight in

231 100 μ L volumes to mice starting at 30 minutes before infection (prophylactic treatment) or 24 hours
232 after infection (day 1, therapeutic treatment). Subsequent doses were administered at
233 approximately the same times each day post-infection.

234 **SARS-CoV-2 challenge studies.** All studies with mice were conducted under the University
235 of North Carolina IACUC approval (20-114). Aged (11- to 12-month-old) female BALB/c mice
236 obtained from Envigo (retired breeders) were acclimated for 7 days in the Biosafety laboratory
237 level 3 prior to any experimentation. Food and water were provided ad libitum, and the animal
238 room maintained a 12-hour light/dark cycle. Prior to inoculation with SARS-CoV-2, animals were
239 anesthetized intraperitoneal with a combination of 50 mg/kg Ketamine and 15 mg/kg Xylazine in
240 50 μ L, and infected intranasally with 1,000 PFU of sequence- and titer-verified SARS-CoV-2 MA10
241 in 50 μ L PBS. Mice were monitored daily for weight loss and disease. At 5 days post-infection,
242 mice were euthanized following sedation by isoflurane and thoracotomy, and lungs were collected
243 for assessments of virus titer, inflammatory cytokines and chemokine levels, histological analysis,
244 and lung congestion score. Lung congestion score was measured using an independently defined
245 scale of 0-4 (0: no congestion; 1: one lobe involved; 2: two lobes involved; 3: three lobes involved;
246 4: all four lobes involved; all scores have 0.5-point intervals). Lung sections used in all experiments
247 for various assessments were as follows: lower right lobe, histology; upper right lobe, RNA; left
248 lobe and central lobe, virus titer. Prior to virus titration and cytokine analysis, the lung lobes were
249 homogenized with glass beads in 1.0 mL PBS, clarified by centrifugation and stored at -80°C.
250 Infectious virus titers were quantified by plaque assay on Vero E6 cells and calculated at PFU/mL
251 of homogenized tissue.

252 **Cytokine Analysis.** Homogenized lung samples were subjected to cytokine and chemokine
253 analysis using the Bio-Rad Mouse Cytokine 23-plex assay (Cat # M60009RDPD) per the
254 manufacturer's protocol. Cytokine assays were performed in non-inactivated samples at BSL3.
255 The data were analyzed on a Luminex MAGPIX machine, and cytokine concentrations in the lung
256 homogenates were extrapolated using the provided standards.

257 **Histological analysis.** Lung tissues from the lower right lobe were fixed for a minimum of 7
258 days in 10% formalin, paraffin embedded, sectioned, and stained with hematoxylin and eosin
259 (H&E). H&E sections were submitted for graded blindly for vasculitis/endotheliitis,
260 Bronchointerstitial pneumonia, and global pneumonia severity score by a board-certified veterinary
261 pathologist. Details on the histology scoring system are provided in the Supplementary Material.

262 **MM3122 in vitro inhibition assays.** Calu-3 cells (5×10^5 cells/well) were seeded in 24-well
263 culture plates in infection medium (DMEM + 1.0 mM Sodium pyruvate, NEAA, 100 U/mL of
264 penicillin, 100 μ g/mL streptomycin, 2.0 mM L-glutamine, 10 mM HEPES, and 2% FBS) and
265 incubated overnight at 37°C and 5% CO₂. After 24 h, media was removed and fresh 250 μ L media
266 was added to each well containing MM3122 or Remdesivir starting at 60 μ M concentration and
267 diluted 3-fold to 20, 6, 2, 0.6 and 0.2 μ M. Media alone, and DMSO were included as negative
268 controls. Next, the cells were transferred to the BSL3 laboratory and 250 μ L of media containing
269 4,000 PFU of SARS-CoV-2 was added for 1 h at 37°C and 5% CO₂. Note, that the final
270 concentration of MM3122 and Remdesivir is 30, 10, 3, 1, 0.3, and 0.1 μ M. After 1 h, the virus
271 inoculum was removed, the cells were washed twice with infection media and fresh infection media
272 containing MM3122, Remdesivir or DMSO was added to each well. At 48 h post-infection, culture
273 supernatant is collected and used to quantify virus titers by plaque assay as described below.

274 **Virus titration assays.** Plaque assays were performed on Vero-hACE2-hTRMPSS2 cells in
275 24-well plates. Lung tissue homogenates or nasal washes were diluted serially by 10-fold, starting
276 at 1:10, in cell infection medium (DMEM + 100 U/mL of penicillin, 100 μ g/mL streptomycin, and 2%
277 FBS). Two hundred and fifty microliters of the diluted virus were added to a single well per dilution
278 per sample. After 1 h at 37°C, the inoculum was aspirated, the cells were washed with PBS, and
279 a 1% methylcellulose overlay in MEM supplemented with 2% FBS was added. Seventy-two to
280 ninety-six hours after virus inoculation, dependent on the virus strain, the cells were fixed with 4%
281 formalin and the monolayer was stained with crystal violet (0.5% w/v in 25% methanol in water)

282 for 30 min at 20°C. The number of plaques were counted and used to calculate the plaque forming
283 units/mL (PFU/mL).

284

285 **ACKNOWLEDGEMENTS**

286 This study was supported by the NIH (NIAID Center of Excellence for Influenza Research and
287 Response (CEIRR)) contract 75N93021C00016 and R01 AI169022 to A.C.M.B and by
288 Washington University School of Medicine, Siteman Cancer Center grant SCC P30CA091842
289 and Barnes Jewish Hospital Foundation award BJHF 4984 to J.W.J. We also acknowledge
290 preclinical services provided by the National Institute of Allergy and Infectious Diseases, National
291 Institutes of Health, Department of Health and Human Services, under contract
292 HHSN272201700036I/75N93020F00001 to the University of North Carolina-Chapel Hill.

293

294 **AUTHOR CONTRIBUTIONS**

295 T.L.B. performed the *in vitro* inhibition studies on Calu-3 cells. E.J.F., S.R.L., K.G., R.S.B,
296 R.L.G. performed all the *in vivo* mouse studies with MM3122 and SARS-CoV-2. B.V.T performed
297 the histology experiments. M.M. synthesized the MM3122 compound. T.L.B., A.C.M.B., R.L.G.,
298 R.S.B., J.W.J. analyzed the data. A.C.M.B. performed the statistical analysis. A.C.M.B. had
299 unrestricted access to all the data. A.C.M.B, J.W.J. provided key reagents, supervised
300 experiments, and acquired funding. A.C.M.B. and J.W.J. wrote the manuscript and all authors
301 reviewed and edited the final version. All authors agreed to submit the manuscript, read, and
302 approved the final draft, and take full responsibility of its content.

303

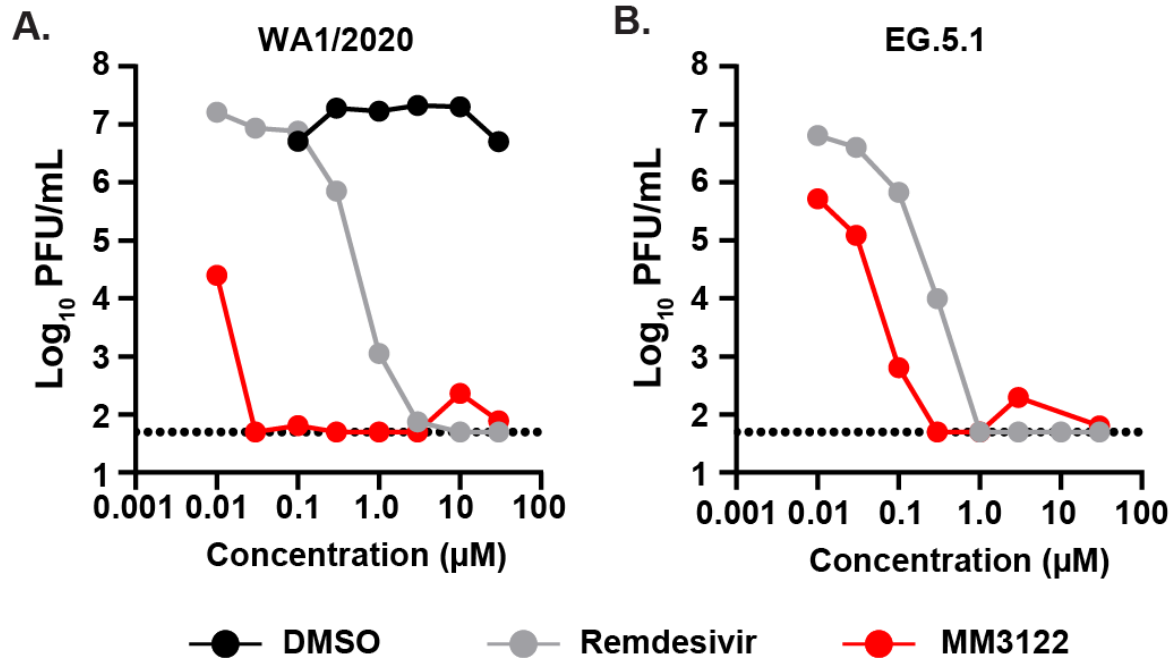
304 **DECLARATION OF INTERESTS**

305 The Boon laboratory has received unrelated funding support in sponsored research
306 agreements from AI Therapeutics, GreenLight Biosciences Inc., Moderna Inc., and Nano targeting
307 & Therapy Biopharma Inc. The Boon laboratory has received funding support from AbbVie Inc.,

308 for the commercial development of SARS-CoV-2 mAb. R.S.B. is a member of the advisory board
309 of VaxArt and Invivyd and has collaborations with Takeda, Janssen Pharmaceuticals, Pfizer,
310 Moderna, Ridgeback Biosciences, and Gilead that are unrelated to this work. J.W.J. has a patent
311 application covering the MM3122 compound. R.S.B. and S.R.L. hold a patent on the MA10 strain
312 of SARS-CoV-2.

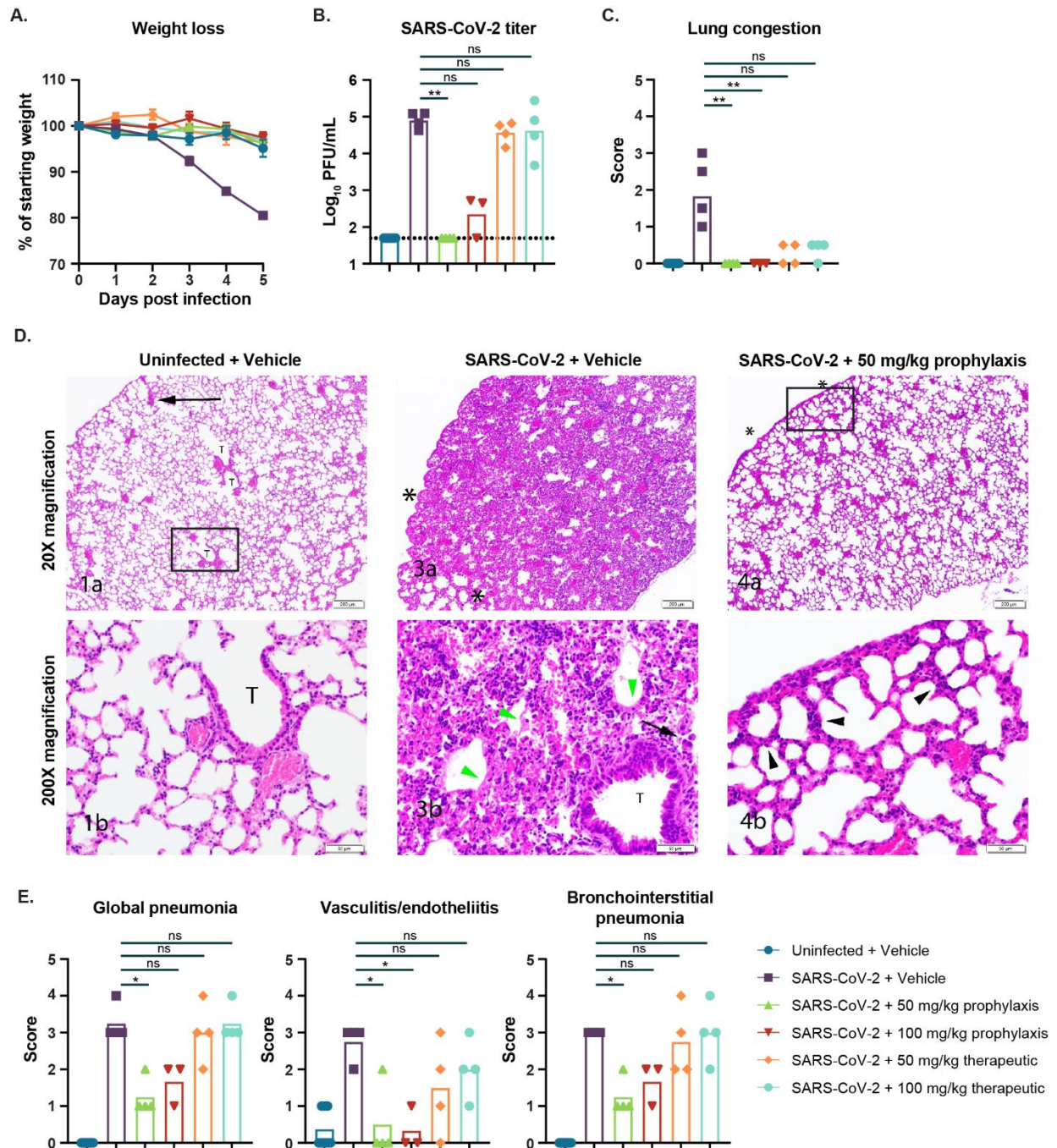
313 **FIGURE AND FIGURE LEGENDS**

314



315

316 **Figure 1: The TMPRSS2 inhibitor MM3122 inhibits replication of authentic SARS-CoV-2 and**
317 **variants.** Calu-3 cells, plated in 24-well plates, were infected with 4,000 PFU of A) WA1/2020
318 and B) EG.5.1 strains of SARS-CoV-2 for one hour at 37°C. After two washes, the cells were
319 incubated for 48 hours in media with different concentrations of MM3122 (red symbol), Remdesivir
320 (grey symbols), or DMSO (black symbols) as the positive and negative controls respectively.
321 Infectious virus titer in the supernatant of the wells 48 hours after infection with SARS-CoV-2. The
322 results are the average of 3 independently repeated assays. The dotted line is the limit of
323 detection.



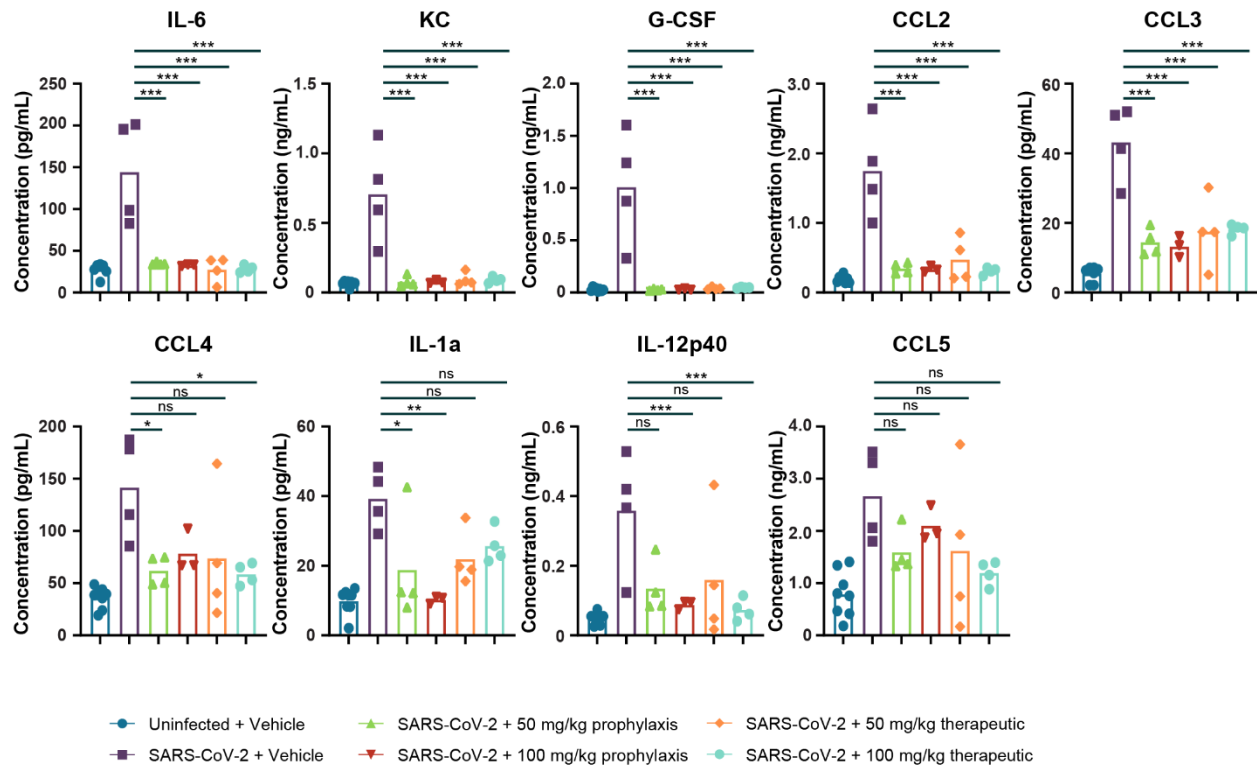
324

Figure 2

325 **Figure 2: MM3122 protects mice against SARS-CoV-2 disease in mice.** Eleven- to twelve-

326 month-old female mice received MM3122 30 minutes before and 24 hours after intranasal

327 inoculation with 1,000 PFU of MA10. **(A)** Weight loss was measured daily for five days. **(B)**
328 Infectious virus titer in left lung lobe 5 days after infection. **(C)** Lung congestion score 5 days after
329 infection. **(D)** Representative images and magnifications of H&E sections of lungs from uninfected
330 and vehicle control treated mice (left panel), SARS-CoV-2 infected, and vehicle control treated
331 mice (middle panels), and MM3122 treated and SARS-CoV-2 infected mice (right panels). **(E)**
332 Global pneumonia, vasculitis and endotheliitis, and bronchointerstitial pathology scores of these
333 same animals. All data was analyzed by a non-parametric one-way ANOVA (Kruskal-Wallis) with
334 multiple comparisons corrects against the SARS-CoV-2 + vehicle group. The dotted line is the
335 limit of detection. Each data point is an individual mouse, and the data are from a single
336 experiment with 3-4 mice per group. ** = $P < 0.01$, ns = not significant.



337

Figure 3

338 **Figure 3: Prophylactic and therapeutic administration of MM3122 reduces inflammation in**
339 **mice.** Eleven- to twelve-month-old female mice received MM3122 30 minutes before and 24
340 hours after intranasal inoculation with 1,000 PFU of SARS-CoV-2 MA10. Cytokine and chemokine
341 concentrations in left lung lobe homogenates collected from these same animals. Data was
342 analyzed by a parametric ordinary one-way ANOVA with multiple comparisons corrected against
343 the SARS-CoV-2 + vehicle group. Each data point is an individual mouse, and the data are from
344 a single experiment with 3-4 mice per group. * = $P < 0.05$, ** = $P < 0.01$, *** = $P < 0.001$, ns = not
345 significant.

346 **Table 1: Protease selectivity profile of MM3122, Camostat and Nafamostat tested against**
 347 **a panel of 53 serine and cysteine proteases.**

Protease	MM3122 IC ₅₀ (M)	Camostat IC ₅₀ (M)	Nafamostat IC ₅₀ (M)	Protease	MM3122 IC ₅₀ (M)	Camostat IC ₅₀ (M)	Nafamostat IC ₅₀ (M)
Serine Proteases				Cysteine Proteases			
HGFA	3.20E-08	>2.00E-05	1.58E-07	Cathepsin B	>2.00E-05	>2.00E-05	>2.00E-05
Matriptase	3.10E-10	7.00E-09	5.00E-11	Cathepsin C	1.393E-06	>2.00E-05	>2.00E-05
Hepsin	1.90E-10	7.00E-09	9.00E-10	Cathepsin H	>2.00E-05	>2.00E-05	>2.00E-05
Factor Xa	7.00E-07	>2.00E-05	4.57E-06	Cathepsin K	>2.00E-05	>2.00E-05	>2.00E-05
Thrombin	>2.00E-05	>2.00E-05	5.02E-06	Cathepsin L	1.28E-05	>2.00E-05	>2.00E-05
TMPRSS2	3.40E-10	1.50E-08	1.40E-10	Cathepsin S	5.857E-07	>2.00E-05	>2.00E-05
FVIIa	1.21E-05	3.55E-06	2.75E-07	Cathepsin V	>2.00E-05	>2.00E-05	>2.00E-05
FXa	1.08E-07	9.91E-06	1.11E-06	SARS-CoV-2-Mpro	>2.00E-05	ND	ND
FXIa	1.76E-06	3.46E-09	8.56E-10	SARS-CoV-2-P1pro	>2.00E-05	ND	ND
Kallikrein 1	1.29E-07	>1.00E-05	2.39E-06	Papain	1.13E-06	>2.00E-05	>2.00E-05
Kallikrein 5	6.81E-07	1.01E-06	6.37E-07	Calpain 1	>2.00E-05	>2.00E-05	>2.00E-05
Kallikrein 7	>2.00E-05	>2.00E-05	>2.00E-05	Caspase 1	>2.00E-05	>2.00E-05	>2.00E-05
Kallikrein 12	>2.00E-05	1.31E-06	3.59E-07	Caspase 2	>2.00E-05	>2.00E-05	>2.00E-05
Kallikrein 13	1.14E-05	8.45E-07	3.02E-07	Caspase 3	>2.00E-05	>2.00E-05	>2.00E-05
Kallikrein 14	6.09E-07	9.99E-07	2.15E-09	Caspase 4	>2.00E-05	>2.00E-05	>2.00E-05
Matriptase-2	2.03E-09	7.80E-09	<5.08E-10	Caspase 5	>2.00E-05	>2.00E-05	>2.00E-05
Plasma Kallikrein	8.06E-09	8.36E-10	<5.08E-10	Caspase 6	>2.00E-05	>2.00E-05	>2.00E-05
Plasmin	7.40E-08	5.62E-09	1.04E-09	Caspase 7	>2.00E-05	>2.00E-05	>2.00E-05
Proteinase A	1.45E-06	>2.00E-05	>2.00E-05	Caspase 8	>2.00E-05	>2.00E-05	>2.00E-05
Proteinase K	1.13E-07	>2.00E-05	>2.00E-05	Caspase 9	>2.00E-05	>2.00E-05	>2.00E-05
Trypsin	<1.02E-09	5.24E-10	<5.08E-10	Caspase 10	>2.00E-05	>2.00E-05	>2.00E-05
Chymotrypsin	>2.00E-05	>2.00E-05	>2.00E-05	Caspase 11	>2.00E-05	>2.00E-05	>2.00E-05
Tryptase b2	3.24E-09	<5.08E-10	<5.08E-10	Caspase 14	>2.00E-05	>2.00E-05	>2.00E-05
Tryptase g1	4.30E-09	<5.08E-10	<5.08E-10				
Urokinase	1.29E-05	1.64E-08	<5.08E-10				
Elastase	>2.00E-05	>2.00E-05	>2.00E-05				
Chymase	>2.00E-05	>2.00E-05	>2.00E-05				
Furin	>2.00E-05	ND	ND				

348

349 Green is IC₅₀ from 0.05 to 10 nM, blue is 10 nM to 1 μM, and yellow is 1 to 100 μM.

350 **SUPPLEMENTARY INFORMATION**

351 **Scoring criteria for Global pneumonia severity.**

Grade	Criteria
Normal = 0	The lung is considered to be within normal limits, under the conditions of the study and considering the age, sex, and strain of the animal
Minimal = 1	≤ 25% of lung affected
Mild = 2	26-50% of lung affected
Moderate = 3	51-79% of lung affected
Marked = 4	≥ 80% of lung affected

352

353

354 **Scoring criteria for Vasculitis / Endotheliitis.**

Grade	Criteria
Normal = 0	No significant microscopic changes present above background lesions if any.
Minimal = 1	Multifocal, scattered, individual infiltrates of inflammatory cells are present along the surface, below the endothelium, or within the tunica media or tunica adventitia of rare vessels.
Mild = 2	Infiltrates of small numbers of individual to occasional focal aggregates of inflammatory cells are present along the surface, below the endothelium, or within the tunica media or tunica adventitia of multiple vessels. There is rare leukocytoclastic vasculitis.
Moderate = 3	Infiltrates of variable numbers of inflammatory cells are present along the surface, below the endothelium, or within the tunica media or tunica adventitia of the majority of vessels. Focal aggregates are common within the endothelium narrowing the lumen and there is occasional leukocytoclastic vasculitis.
Marked = 4	Infiltrates of focally large numbers of inflammatory cells are present along the surface, below the endothelium, or within the tunica media or tunica adventitia of almost all vessels. Large aggregates are common within the endothelium narrowing the lumen and there is common leukocytoclastic vasculitis.

355

356 **Scoring criteria for Bronchointerstitial pneumonia.**

Grade	Criteria
Normal = 0	No significant microscopic changes present above background lesions, if any.
Minimal = 1	Affected alveolar septa are visibly but minimally thickened and there are only small amounts of hyaline membrane formation, edema, fibrin deposition, or hemorrhage within bronchioles and alveolar airways, with little loss of total airway space.
Mild = 2	Affected alveolar septa are mildly thickened and hyaline membrane formation, edema, fibrin deposition, or hemorrhage are commonly observed within alveolar spaces and bronchioles. Focal areas of atelectasis and consolidation may be present.
Moderate = 3	Infiltrates of inflammatory cells are present within the septa and spaces of most alveoli. Affected alveolar septa are moderately thickened, and hyaline membrane formation, edema, fibrin deposition, or hemorrhage are frequently observed within alveolar spaces or bronchioles along with prominent loss of airspace. Multifocal and regional areas of atelectasis and consolidation are present.
Marked = 4	Infiltrates of large numbers of inflammatory cells are present within the septa and spaces of most alveoli. Affected alveolar septa are markedly thickened, and hyaline membrane formation, edema, fibrin deposition, or hemorrhage within alveolar airways and bronchioles are frequently observed. Large areas of atelectasis and consolidation are present.

357

358 REFERENCES

- 359 1. Shoichet BK, Craik CS. Preparing for the next pandemic. *Science*. 2023;382(6671):649-50. Epub
360 20231109. doi: 10.1126/science.adk5868. PubMed PMID: 37943911.
- 361 2. Sheahan TP, Sims AC, Zhou S, Graham RL, Pruijssers AJ, Agostini ML, Leist SR, Schäfer A, Dinnon
362 KH, 3rd, Stevens LJ, Chappell JD, Lu X, Hughes TM, George AS, Hill CS, Montgomery SA, Brown AJ,
363 Bluemling GR, Natchus MG, Saindane M, Kolykhalov AA, Painter G, Harcourt J, Tamin A, Thornburg NJ,
364 Swanstrom R, Denison MR, Baric RS. An orally bioavailable broad-spectrum antiviral inhibits SARS-CoV-2
365 in human airway epithelial cell cultures and multiple coronaviruses in mice. *Sci Transl Med*. 2020;12(541).
366 Epub 20200406. doi: 10.1126/scitranslmed.abb5883. PubMed PMID: 32253226; PMCID: PMC7164393.
- 367 3. Sheahan TP, Sims AC, Graham RL, Menachery VD, Gralinski LE, Case JB, Leist SR, Pyrc K, Feng JY,
368 Trantcheva I, Bannister R, Park Y, Babusis D, Clarke MO, Mackman RL, Spahn JE, Palmiotti CA, Siegel D,
369 Ray AS, Cihlar T, Jordan R, Denison MR, Baric RS. Broad-spectrum antiviral GS-5734 inhibits both epidemic
370 and zoonotic coronaviruses. *Sci Transl Med*. 2017;9(396). doi: 10.1126/scitranslmed.aal3653. PubMed
371 PMID: 28659436; PMCID: PMC5567817.
- 372 4. Corbett KS, Edwards DK, Leist SR, Abiona OM, Boyoglu-Barnum S, Gillespie RA, Himansu S, Schäfer
373 A, Ziwawo CT, DiPiazza AT, Dinnon KH, Elbashir SM, Shaw CA, Woods A, Fritch EJ, Martinez DR, Bock KW,
374 Minai M, Nagata BM, Hutchinson GB, Wu K, Henry C, Bahl K, Garcia-Dominguez D, Ma L, Renzi I, Kong WP,
375 Schmidt SD, Wang L, Zhang Y, Phung E, Chang LA, Loomis RJ, Altaras NE, Narayanan E, Metkar M, Presnyak
376 V, Liu C, Louder MK, Shi W, Leung K, Yang ES, West A, Gully KL, Stevens LJ, Wang N, Wrapp D, Doria-Rose
377 NA, Stewart-Jones G, Bennett H, Alvarado GS, Nason MC, Ruckwardt TJ, McLellan JS, Denison MR, Chappell
378 JD, Moore IN, Morabito KM, Mascola JR, Baric RS, Carfi A, Graham BS. SARS-CoV-2 mRNA vaccine design
379 enabled by prototype pathogen preparedness. *Nature*. 2020;586(7830):567-71. Epub 20200805. doi:
380 10.1038/s41586-020-2622-0. PubMed PMID: 32756549; PMCID: PMC7581537.
- 381 5. Rahbar Saadat Y, Hosseiniyan Khatibi SM, Zununi Vahed S, Ardalan M. Host Serine Proteases: A
382 Potential Targeted Therapy for COVID-19 and Influenza. *Front Mol Biosci*. 2021;8:725528. Epub 20210830.
383 doi: 10.3389/fmolb.2021.725528. PubMed PMID: 34527703; PMCID: PMC8435734.
- 384 6. Zhou P, Yang XL, Wang XG, Hu B, Zhang L, Zhang W, Si HR, Zhu Y, Li B, Huang CL, Chen HD, Chen J,
385 Luo Y, Guo H, Jiang RD, Liu MQ, Chen Y, Shen XR, Wang X, Zheng XS, Zhao K, Chen QJ, Deng F, Liu LL, Yan
386 B, Zhan FX, Wang YY, Xiao GF, Shi ZL. A pneumonia outbreak associated with a new coronavirus of
387 probable bat origin. *Nature*. 2020;579(7798):270-3. Epub 20200203. doi: 10.1038/s41586-020-2012-7.
388 PubMed PMID: 32015507; PMCID: PMC7095418.
- 389 7. Hoffmann M, Kleine-Weber H, Schroeder S, Krüger N, Herrler T, Erichsen S, Schiergens TS, Herrler
390 G, Wu NH, Nitsche A, Müller MA, Drosten C, Pöhlmann S. SARS-CoV-2 Cell Entry Depends on ACE2 and
391 TMPRSS2 and Is Blocked by a Clinically Proven Protease Inhibitor. *Cell*. 2020;181(2):271-80.e8. Epub
392 20200305. doi: 10.1016/j.cell.2020.02.052. PubMed PMID: 32142651; PMCID: PMC7102627.
- 393 8. Gomes CP, Fernandes DE, Casimiro F, da Mata GF, Passos MT, Varela P, Mastroianni-Kirsztajn G,
394 Pesquero JB. Cathepsin L in COVID-19: From Pharmacological Evidences to Genetics. *Front Cell Infect
395 Microbiol*. 2020;10:589505. Epub 20201208. doi: 10.3389/fcimb.2020.589505. PubMed PMID: 33364201;
396 PMCID: PMC7753008.
- 397 9. Vaarala MH, Porvari KS, Kellokumpu S, Kyllonen AP, Vihko PT. Expression of transmembrane
398 serine protease TMPRSS2 in mouse and human tissues. *The Journal of pathology*. 2001;193(1):134-40.
399 Epub 2001/02/13. doi: 10.1002/1096-9896(2000)9999:9999<::AID-PATH743>3.0.CO;2-T. PubMed PMID:
400 11169526.
- 401 10. Vaarala MH, Porvari K, Kyllonen A, Lukkarinen O, Vihko P. The TMPRSS2 gene encoding
402 transmembrane serine protease is overexpressed in a majority of prostate cancer patients: detection of
403 mutated TMPRSS2 form in a case of aggressive disease. *Int J Cancer*. 2001;94(5):705-10. Epub 2001/12/18.
404 doi: 10.1002/ijc.1526. PubMed PMID: 11745466.

- 405 11. Afar DE, Vivanco I, Hubert RS, Kuo J, Chen E, Saffran DC, Raitano AB, Jakobovits A. Catalytic
406 cleavage of the androgen-regulated TMPRSS2 protease results in its secretion by prostate and prostate
407 cancer epithelia. *Cancer Res.* 2001;61(4):1686-92. Epub 2001/03/14. PubMed PMID: 11245484.
- 408 12. Damalanka VC, Janetka JW. Recent progress on inhibitors of the type II transmembrane serine
409 proteases, hepsin, matriptase and matriptase-2. *Future Med Chem.* 2019;11(7):743-69. Epub 20190404.
410 doi: 10.4155/fmc-2018-0446. PubMed PMID: 30945556.
- 411 13. Tanabe LM, List K. The role of type II transmembrane serine protease-mediated signaling in
412 cancer. *FEBS J.* 2017;284(10):1421-36. Epub 2016/11/22. doi: 10.1111/febs.13971. PubMed PMID:
413 27870503; PMCID: PMC5432387.
- 414 14. Kuhn N, Bergmann S, Kasnitz N, Lambertz RL, Keppner A, van den Brand JM, Pohlmann S, Weiss S,
415 Hummler E, Hatesuer B, Schughart K. The proteolytic activation of A (H3N2) Influenza virus hemagglutinin
416 is facilitated by different type II transmembrane serine proteases. *Journal of Virology.* 2016. Epub
417 2016/02/19. doi: 10.1128/JVI.02693-15. PubMed PMID: 26889029.
- 418 15. Lucas JM, Heinlein C, Kim T, Hernandez SA, Malik MS, True LD, Morrissey C, Corey E, Montgomery
419 B, Mostaghel E, Clegg N, Coleman I, Brown CM, Schneider EL, Craik C, Simon JA, Bedalov A, Nelson PS. The
420 androgen-regulated protease TMPRSS2 activates a proteolytic cascade involving components of the
421 tumor microenvironment and promotes prostate cancer metastasis. *Cancer Discov.* 2014;4(11):1310-25.
422 Epub 2014/08/15. doi: 10.1158/2159-8290.CD-13-1010. PubMed PMID: 25122198; PMCID: PMC4409786.
- 423 16. Glowacka I, Bertram S, Muller MA, Allen P, Soilleux E, Pfefferle S, Steffen I, Tsegaye TS, He Y, Gnirss
424 K, Niemeyer D, Schneider H, Drosten C, Pohlmann S. Evidence that TMPRSS2 activates the severe acute
425 respiratory syndrome coronavirus spike protein for membrane fusion and reduces viral control by the
426 humoral immune response. *J Virol.* 2011;85(9):4122-34. Epub 2011/02/18. doi: 10.1128/JVI.02232-10.
427 PubMed PMID: 21325420; PMCID: PMC3126222.
- 428 17. Bertram S, Glowacka I, Müller MA, Lavender H, Gnirss K, Nehlmeier I, Niemeyer D, He Y, Simmons
429 G, Drosten C, Soilleux EJ, Jahn O, Steffen I, Pöhlmann S. Cleavage and activation of the severe acute
430 respiratory syndrome coronavirus spike protein by human airway trypsin-like protease. *J Virol.*
431 2011;85(24):13363-72. Epub 20111012. doi: 10.1128/jvi.05300-11. PubMed PMID: 21994442; PMCID:
432 PMC3233180.
- 433 18. Saunders N, Fernandez I, Planchais C, Michel V, Rajah MM, Baquero Salazar E, Postal J, Porrot F,
434 Guivel-Benhassine F, Blanc C, Chauveau-Le Fric G, Martin A, Grzelak L, Oktavia RM, Meola A, Ahouzi O,
435 Hoover-Watson H, Prot M, Delaune D, Cornelissen M, Deijs M, Meriaux V, Mouquet H, Simon-Lorière E,
436 van der Hoek L, Lafaye P, Rey F, Buchrieser J, Schwartz O. TMPRSS2 is a functional receptor for human
437 coronavirus HKU1. *Nature.* 2023;624(7990):207-14. Epub 20231025. doi: 10.1038/s41586-023-06761-7.
438 PubMed PMID: 37879362.
- 439 19. Shirato K, Kawase M, Matsuyama S. Middle East respiratory syndrome coronavirus infection
440 mediated by the transmembrane serine protease TMPRSS2. *J Virol.* 2013;87(23):12552-61. Epub
441 2013/09/13. doi: 10.1128/JVI.01890-13. PubMed PMID: 24027332; PMCID: PMC3838146.
- 442 20. Bertram S, Dijkman R, Habjan M, Heurich A, Gierer S, Glowacka I, Welsch K, Winkler M, Schneider
443 H, Hofmann-Winkler H, Thiel V, Pohlmann S. TMPRSS2 activates the human coronavirus 229E for
444 cathepsin-independent host cell entry and is expressed in viral target cells in the respiratory epithelium. *J*
445 *Virol.* 2013;87(11):6150-60. Epub 2013/03/29. doi: 10.1128/JVI.03372-12. PubMed PMID: 23536651;
446 PMCID: PMC3648130.
- 447 21. Gierer S, Bertram S, Kaup F, Wrensch F, Heurich A, Kramer-Kuhl A, Welsch K, Winkler M, Meyer B,
448 Drosten C, Dittmer U, von Hahn T, Simmons G, Hofmann H, Pohlmann S. The spike protein of the emerging
449 betacoronavirus EMC uses a novel coronavirus receptor for entry, can be activated by TMPRSS2, and is
450 targeted by neutralizing antibodies. *J Virol.* 2013;87(10):5502-11. Epub 2013/03/08. doi:
451 10.1128/JVI.00128-13. PubMed PMID: 23468491; PMCID: PMC3648152.

- 452 22. Beaulieu A, Gravel É, Cloutier A, Marois I, Colombo É, Désilets A, Verreault C, Leduc R, Marsault É,
453 Richter MV. Matriptase Proteolytically Activates Influenza Virus and Promotes Multicycle Replication in
454 the Human Airway Epithelium. *Journal of Virology*. 2013;87(8):4237-51. doi: doi:10.1128/jvi.03005-12.
- 455 23. Whittaker GR, Straus MR. Human matriptase/ST 14 proteolytically cleaves H7N9 hemagglutinin
456 and facilitates the activation of influenza A/Shanghai/2/2013 virus in cell culture. *Influenza Other Respir*
457 *Viruses*. 2020;14(2):189-95. Epub 2019/12/11. doi: 10.1111/irv.12707. PubMed PMID: 31820577; PMCID:
458 PMC7040964.
- 459 24. Baron J, Tarnow C, Mayoli-Nussle D, Schilling E, Meyer D, Hammami M, Schwalm F, Steinmetzer
460 T, Guan Y, Garten W, Klenk HD, Bottcher-Friebertshäuser E. Matriptase, HAT, and TMPRSS2 activate the
461 hemagglutinin of H9N2 influenza A viruses. *J Virol*. 2013;87(3):1811-20. Epub 2012/11/30. doi:
462 10.1128/JVI.02320-12. PubMed PMID: 23192872; PMCID: PMC3554176.
- 463 25. Bottcher E, Matrosovich T, Beyerle M, Klenk HD, Garten W, Matrosovich M. Proteolytic activation
464 of influenza viruses by serine proteases TMPRSS2 and HAT from human airway epithelium. *J Virol*.
465 2006;80(19):9896-8. Epub 2006/09/16. doi: 10.1128/JVI.01118-06. PubMed PMID: 16973594; PMCID:
466 PMC1617224.
- 467 26. Bottcher-Friebertshäuser E, Freuer C, Sielaff F, Schmidt S, Eickmann M, Uhlendorff J, Steinmetzer
468 T, Klenk HD, Garten W. Cleavage of influenza virus hemagglutinin by airway proteases TMPRSS2 and HAT
469 differs in subcellular localization and susceptibility to protease inhibitors. *Journal of Virology*.
470 2010;84(11):5605-14. Epub 2010/03/20. doi: 10.1128/JVI.00140-10. PubMed PMID: 20237084; PMCID:
471 2876594.
- 472 27. Paszti-Gere E, Czimmermann E, Ujhelyi G, Balla P, Maiwald A, Steinmetzer T. In vitro
473 characterization of TMPRSS2 inhibition in IPEC-J2 cells. *J Enzyme Inhib Med Chem*. 2016;31(sup2):123-9.
474 Epub 2016/06/10. doi: 10.1080/14756366.2016.1193732. PubMed PMID: 27277342.
- 475 28. Bertram S, Glowacka I, Blazejewska P, Soilleux E, Allen P, Danisch S, Steffen I, Choi SY, Park Y,
476 Schneider H, Schughart K, Pohlmann S. TMPRSS2 and TMPRSS4 facilitate trypsin-independent spread of
477 influenza virus in Caco-2 cells. *J Virol*. 2010;84(19):10016-25. Epub 2010/07/16. doi: 10.1128/JVI.00239-
478 10. PubMed PMID: 20631123; PMCID: PMC2937781.
- 479 29. Hatesuer B, Bertram S, Mehnert N, Bahgat MM, Nelson PS, Pohlmann S, Schughart K. Tmprss2 is
480 essential for influenza H1N1 virus pathogenesis in mice. *PLoS Pathog*. 2013;9(12):e1003774. Epub
481 2013/12/19. doi: 10.1371/journal.ppat.1003774. PubMed PMID: 24348248; PMCID: PMC3857797.
- 482 30. Lambertz RLO, Gerhäuser I, Nehlmeier I, Gartner S, Winkler M, Leist SR, Kollmus H, Pohlmann S,
483 Schughart K. H2 influenza A virus is not pathogenic in Tmprss2 knock-out mice. *Virology*. 2020;17(1):56.
484 Epub 2020/04/24. doi: 10.1186/s12985-020-01323-z. PubMed PMID: 32321537; PMCID: PMC7178614.
- 485 31. Tarnow C, Engels G, Arendt A, Schwalm F, Sediri H, Preuss A, Nelson PS, Garten W, Klenk HD,
486 Gabriel G, Bottcher-Friebertshäuser E. TMPRSS2 is a host factor that is essential for pneumotropism and
487 pathogenicity of H7N9 influenza A virus in mice. *J Virol*. 2014;88(9):4744-51. Epub 2014/02/14. doi:
488 10.1128/jvi.03799-13. PubMed PMID: 24522916; PMCID: 3993819.
- 489 32. Abe M, Tahara M, Sakai K, Yamaguchi H, Kanou K, Shirato K, Kawase M, Noda M, Kimura H,
490 Matsuyama S, Fukuhara H, Mizuta K, Maenaka K, Ami Y, Esumi M, Kato A, Takeda M. TMPRSS2 is an
491 activating protease for respiratory parainfluenza viruses. *J Virol*. 2013;87(21):11930-5. Epub 2013/08/21.
492 doi: 10.1128/jvi.01490-13. PubMed PMID: 23966399; PMCID: PMC3807344.
- 493 33. Yang H, Lin X, Yu Q, Awadasseid A, Zhang W. Repurposing and discovery of transmembrane serine
494 protease 2 (TMPRSS2) inhibitors as prophylactic therapies for new coronavirus disease 2019 (COVID-19).
495 *Pharmazie*. 2023;78(11):217-24. doi: 10.1691/ph.2023.3578. PubMed PMID: 38178286.
- 496 34. Meyer D, Sielaff F, Hammami M, Bottcher-Friebertshäuser E, Garten W, Steinmetzer T.
497 Identification of the first synthetic inhibitors of the type II transmembrane serine protease TMPRSS2
498 suitable for inhibition of influenza virus activation. *Biochem J*. 2013;452(2):331-43. Epub 2013/03/27. doi:
499 10.1042/BJ20130101. PubMed PMID: 23527573.

- 500 35. Colombo E, Duchene D, Desilets A, Beaulieu A, Gravel E, Najmanovich R, Richter M, Leduc R,
501 Marsault E. New matriptase inhibitors as a potential treatment against influenza. Abstracts of Papers of
502 the American Chemical Society. 2013;245. PubMed PMID: ISI:000324303602432.
- 503 36. Colombo E, Desilets A, Hassanzadeh M, Lemieux G, Marois I, Cliche D, Delbrouck JA, Murza A, Jean
504 F, Marsault E, Richter MV, Leduc R, Boudreault PL. Optimization of Ketobenzothiazole-Based Type II
505 Transmembrane Serine Protease Inhibitors to Block H1N1 Influenza Virus Replication. *ChemMedChem*.
506 2023:e202300458. Epub 20231021. doi: 10.1002/cmdc.202300458. PubMed PMID: 37864572.
- 507 37. Pilgram O, Keils A, Benary GE, Müller J, Merkl S, Ngaha S, Huber S, Chevillard F, Harbig A, Magdolen
508 V, Heine A, Böttcher-Friebertshäuser E, Steinmetzer T. Improving the selectivity of 3-
509 amidinophenylalanine-derived matriptase inhibitors. *European Journal of Medicinal Chemistry*.
510 2022;238:114437. doi: <https://doi.org/10.1016/j.ejmech.2022.114437>.
- 511 38. Bestle D, Heindl MR, Limburg H, van TVL, Pilgram O, Moulton H, Stein DA, Harges K, Eickmann M,
512 Dolnik O, Rohde C, Klenk H-D, Garten W, Steinmetzer T, Böttcher-Friebertshäuser E. TMPRSS2 and furin
513 are both essential for proteolytic activation of SARS-CoV-2 in human airway cells. *Life Science Alliance*.
514 2020;3(9):e202000786. doi: 10.26508/lsa.202000786.
- 515 39. Mahoney M, Damalanka VC, Tartell MA, Chung DH, Lourenço AL, Pwee D, Mayer Bridwell AE,
516 Hoffmann M, Voss J, Karmakar P, Azouz NP, Klingler AM, Rothlauf PW, Thompson CE, Lee M, Klampfer L,
517 Stallings CL, Rothenberg ME, Pöhlmann S, Whelan SPJ, O'Donoghue AJ, Craik CS, Janetka JW. A novel class
518 of TMPRSS2 inhibitors potently block SARS-CoV-2 and MERS-CoV viral entry and protect human epithelial
519 lung cells. *Proc Natl Acad Sci U S A*. 2021;118(43). doi: 10.1073/pnas.2108728118. PubMed PMID:
520 34635581; PMCID: PMC8694051.
- 521 40. Fraser BJ, Beldar S, Seitova A, Hutchinson A, Mannar D, Li Y, Kwon D, Tan R, Wilson RP, Leopold K,
522 Subramaniam S, Halabelian L, Arrowsmith CH, Benard F. Structure and activity of human TMPRSS2
523 protease implicated in SARS-CoV-2 activation. *Nat Chem Biol*. 2022;18(9):963-71. Epub 20220608. doi:
524 10.1038/s41589-022-01059-7. PubMed PMID: 35676539.
- 525 41. Hoffmann M, Hofmann-Winkler H, Smith JC, Kruger N, Arora P, Sorensen LK, Sogaard OS,
526 Hasselstrom JB, Winkler M, Hempel T, Raich L, Olsson S, Danov O, Jonigk D, Yamazoe T, Yamatsuta K,
527 Mizuno H, Ludwig S, Noe F, Kjolby M, Braun A, Sheltzer JM, Pöhlmann S. Camostat mesylate inhibits SARS-
528 CoV-2 activation by TMPRSS2-related proteases and its metabolite GBPA exerts antiviral activity.
529 *EBioMedicine*. 2021;65:103255. Epub 2021/03/08. doi: 10.1016/j.ebiom.2021.103255. PubMed PMID:
530 33676899; PMCID: PMC7930809.
- 531 42. Shapira T, Monreal IA, Dion SP, Buchholz DW, Imbiakha B, Olmstead AD, Jager M, Désilets A, Gao
532 G, Martins M, Vandal T, Thompson CAH, Chin A, Rees WD, Steiner T, Nabi IR, Marsault E, Sahler J, Diel DG,
533 Van de Walle GR, August A, Whittaker GR, Boudreault P-L, Leduc R, Aguilar HC, Jean F. A TMPRSS2 inhibitor
534 acts as a pan-SARS-CoV-2 prophylactic and therapeutic. *Nature*. 2022;605(7909):340-8. doi:
535 10.1038/s41586-022-04661-w.
- 536 43. Lin HXJ, Cho S, Meyyur Aravamudan V, Sanda HY, Palraj R, Molton JS, Venkatachalam I. Remdesivir
537 in Coronavirus Disease 2019 (COVID-19) treatment: a review of evidence. *Infection*. 2021;49(3):401-10.
538 Epub 20210102. doi: 10.1007/s15010-020-01557-7. PubMed PMID: 33389708; PMCID: PMC7778417.
- 539 44. Shrimp JH, Kales SC, Sanderson PE, Simeonov A, Shen M, Hall MD. An Enzymatic TMPRSS2 Assay
540 for Assessment of Clinical Candidates and Discovery of Inhibitors as Potential Treatment of COVID-19. *ACS*
541 *Pharmacology & Translational Science*. 2020;3(5):997-1007. doi: 10.1021/acscptsci.0c00106.
- 542 45. Walmsley T, Rose A, John R, Wei D, Hlávka JP, Machado J, Byrd K. Macroeconomic consequences
543 of the COVID-19 pandemic. *Economic Modelling*. 2023;120:106147. doi:
544 <https://doi.org/10.1016/j.econmod.2022.106147>.
- 545 46. Msemburi W, Karlinsky A, Knutson V, Aleshin-Guendel S, Chatterji S, Wakefield J. The WHO
546 estimates of excess mortality associated with the COVID-19 pandemic. *Nature*. 2023;613(7942):130-7.
547 doi: 10.1038/s41586-022-05522-2.

- 548 47. Agrawal V, Sood N, Whaley CM. The Impact of the Global COVID-19 Vaccination Campaign on All-
549 Cause Mortality. National Bureau of Economic Research Working Paper Series. 2023;No. 31812. doi:
550 10.3386/w31812.
- 551 48. Hall FC, Cheriyan J, Cope AP, Galloway J, Wilkinson I, Bond S, Norton S, Banham-Hall E, Bayes H,
552 Kostapanos M, Nodale M, Petchey WG, Sheeran T, Underwood J, Jayne DR, Group T-RI. Efficacy and safety
553 of baricitinib or ravulizumab in adult patients with severe COVID-19 (TACTIC-R): a randomised, parallel-
554 arm, open-label, phase 4 trial. *Lancet Respir Med.* 2023;11(12):1064-74. Epub 20231114. doi:
555 10.1016/S2213-2600(23)00376-4. PubMed PMID: 37977159; PMCID: PMC10682367.
- 556 49. Dastan F, Jamaati H, Barati S, Varmazyar S, Yousefian S, Niknami E, Tabarsi P. The effects of
557 combination-therapy of tocilizumab and baricitinib on the management of severe COVID-19 cases: a
558 randomized open-label clinical trial. *Front Pharmacol.* 2023;14:1265541. Epub 20231019. doi:
559 10.3389/fphar.2023.1265541. PubMed PMID: 37927607; PMCID: PMC10620525.
- 560 50. Song W, Sun S, Feng Y, Liu L, Gao T, Xian S, Chen J. Efficacy and safety of baricitinib in patients
561 with severe COVID-19: A systematic review and meta-analysis. *Medicine (Baltimore).*
562 2023;102(48):e36313. doi: 10.1097/MD.00000000000036313. PubMed PMID: 38050265; PMCID:
563 PMC10695502.
- 564 51. Fuentes-Prior P. Priming of SARS-CoV-2 S protein by several membrane-bound serine proteinases
565 could explain enhanced viral infectivity and systemic COVID-19 infection. *J Biol Chem.* 2021;296:100135.
566 Epub 20201206. doi: 10.1074/jbc.REV120.015980. PubMed PMID: 33268377; PMCID: PMC7834812.
- 567 52. Chen RE, Zhang X, Case JB, Winkler ES, Liu Y, VanBlargan LA, Liu J, Errico JM, Xie X, Suryadevara N,
568 Gilchuk P, Zost SJ, Tahan S, Droit L, Turner JS, Kim W, Schmitz AJ, Thapa M, Wang D, Boon ACM, Presti RM,
569 O'Halloran JA, Kim AHJ, Deepak P, Pinto D, Fremont DH, Crowe JE, Jr., Corti D, Virgin HW, Ellebedy AH, Shi
570 PY, Diamond MS. Resistance of SARS-CoV-2 variants to neutralization by monoclonal and serum-derived
571 polyclonal antibodies. *Nat Med.* 2021. Epub 2021/03/06. doi: 10.1038/s41591-021-01294-w. PubMed
572 PMID: 33664494.
- 573 53. Zang R, Gomez Castro MF, McCune BT, Zeng Q, Rothlauf PW, Sonnek NM, Liu Z, Brulois KF, Wang
574 X, Greenberg HB, Diamond MS, Ciorba MA, Whelan SPJ, Ding S. TMPRSS2 and TMPRSS4 promote SARS-
575 CoV-2 infection of human small intestinal enterocytes. *Sci Immunol.* 2020;5(47). Epub 2020/05/15. doi:
576 10.1126/sciimmunol.abc3582. PubMed PMID: 32404436.
- 577 54. Leist SR, Dinnon KH, 3rd, Schäfer A, Tse LV, Okuda K, Hou YJ, West A, Edwards CE, Sanders W,
578 Fritch EJ, Gully KL, Scobey T, Brown AJ, Sheahan TP, Moorman NJ, Boucher RC, Gralinski LE, Montgomery
579 SA, Baric RS. A Mouse-Adapted SARS-CoV-2 Induces Acute Lung Injury and Mortality in Standard
580 Laboratory Mice. *Cell.* 2020;183(4):1070-85.e12. Epub 20200923. doi: 10.1016/j.cell.2020.09.050.
581 PubMed PMID: 33031744; PMCID: PMC7510428.
- 582 55. Dinnon KH, 3rd, Leist SR, Okuda K, Dang H, Fritch EJ, Gully KL, De la Cruz G, Evangelista MD,
583 Asakura T, Gilmore RC, Hawkins P, Nakano S, West A, Schäfer A, Gralinski LE, Everman JL, Sajuthi SP,
584 Zweigart MR, Dong S, McBride J, Cooley MR, Hines JB, Love MK, Groshong SD, VanSchoiack A, Phelan SJ,
585 Liang Y, Hether T, Leon M, Zumwalt RE, Barton LM, Duval EJ, Mukhopadhyay S, Stroberg E, Borczuk A,
586 Thorne LB, Sakthivel MK, Lee YZ, Hagood JS, Mock JR, Seibold MA, O'Neal WK, Montgomery SA, Boucher
587 RC, Baric RS. SARS-CoV-2 infection produces chronic pulmonary epithelial and immune cell dysfunction
588 with fibrosis in mice. *Sci Transl Med.* 2022;14(664):eabo5070. Epub 20220928. doi:
589 10.1126/scitranslmed.abo5070. PubMed PMID: 35857635; PMCID: PMC9273046.